Supporting information for

One Arrow Two Eagle: Design and Synthesis of "All-in-One" Nanoscale Cu-IR825 Nanoparticles for Photothermally-Augmented Chemodynamic therapy

Wei Wang,[†,a] Dan Luo,[†,a] Yuzi Huang,[a] Yuting Zhang,[a] Peng Geng,[a,*] Qiancheng Jin,[a] Wenquan Huang,[b,*] and Shuzhang Xiao,[a,c,*]

[a] College of Materials and Chemical Engineering, Key Laboratory of Inorganic Nonmetallic Crystalline and Energy Conversion Materials, China Three Gorges University, Yichang 443002, Hubei, China.

[b] College of Medicine and Health Science, China Three Gorges University, Yichang, China.

[c] Hubei Three Gorges Laboratory, Yichang 443007, Hubei, China

[†] These authors contributed equally to this work.

* Corresponding authors. E-mail address: gengpeng@ctgu.edu.cn (P. Geng); huangwenquan@ctgu.edu.cn (W. Huang); shuzhangxiao@ctgu.edu.cn (S. Xiao).

1. Experiment section

1.1 Experimental materials

$CuCl_2 \cdot 2H_2O$, analytical grade, Shanghai Macklin Biochemical Technology Co., Ltd.; IR825, 95%, Shanghai Yuanye Biotechnology Co., Ltd.; Polyvinylpyrrolidone (PVP-K30), analytical grade, Shanghai Macklin Biochemical Technology Co., Ltd.; CH_3OH, analytical grade, Shanghai Macklin Biochemical Technology Co., Ltd.; N,N-Dimethylformamide, analytical grade, Shanghai Macklin Biochemical Technology Co., Ltd.; Triethylamine, analytical grade, Tianjin Kemiou Chemical Reagent Co., Ltd.; CH_3CH_2OH, analytical grade, Shanghai Aladdin Biochemical Technology Co., Ltd.; H_2O_2, 30%, Tianjin Kemiou Chemical Reagent Co., Ltd.; Methylene blue (MB), analytical grade, Shanghai Macklin Biochemical Technology Co., Ltd.; Phosphate-buffered saline (PBS), analytical grade, Shanghai Macklin Biochemical Technology Co., Ltd.

1.2 Experimental instruments

85-2 Thermostatic Heating Magnetic Stirrer (Shanghai Meiyingpu Instrument Manufacturing Co., Ltd.); HJ-6(A) Digital Multi-head Thermostatic Magnetic Stirrer (Changzhou Runhua Electric Co., Ltd.); TG16-WS Centrifuge (Hunan Xiangyi Laboratory Instrument Development Co., Ltd.); PX225DHZ Electronic Analytical Balance (Ohaus Instruments); DHG-9053A Electric Heating

Constant Temperature Forced Air Drying Oven (Shanghai Qixin Scientific Instrument Co., Ltd.); JSM-7500F Scanning Electron Microscope (JEOL, Japan); AXIS Supra X-ray Photoelectron Spectrometer (Shimadzu, Japan); Fourier Transform Infrared Spectrometer (PE, USA); Shimadzu UV-2600 UV-Visible Spectrophotometer (Shimadzu, Japan); Hitachi F-4600 Fluorescence Spectrometer (Hitachi, Japan); NANOTRAC WAVE II Nanoparticle Size and Zeta Potential Analyzer (Microtrac, USA); HM-TPK20-3AQF/W Handheld Thermal Imager (Hangzhou Weiying Software Co., Ltd.); 808-A Semiconductor Laser (Shanghai Xilong Optoelectronic Technology Co., Ltd.).

1.3 Photothermal efficiency calculation

Cu-IR825 (100 μL) aqueous dispersion was irradiated with an 808 nm laser. The dispersion was irradiated for 600 seconds, allowing the temperature to stabilize at T_{max} = 60.1°C. The laser was then turned off, and the temperature was allowed to cool to room temperature (T_{sur} = 32°C). The photothermal conversion efficiency was calculated using an improved method based on the report by Roper.

$$\eta_T = \frac{hA(T_{max} - T_{surr}) - Q_{dis}}{I\left(1 - 10^{-A_{808}}\right)}$$

In this equation, h, A, and I represent the heat transfer coefficient, the surface area of the container, and the laser power, respectively. The absorbance (A_{808}) was calculated to be 0.65. The term hA can be calculated using the following equation:

$$\tau_s = \frac{m_{H2O}C_{H2O}}{hA}$$

Where τs is the system's time constant (159.2 s); m_{H2O} and C_{H2O} are the mass (0.1 g) and specific heat (4.2 $J \cdot g^{-1}$) of deionized water. Under similar conditions, water was used to independently test Q_{dis}, which was found to be 0.0041.

Therefore, the photothermal conversion efficiency (η_T) of Cu-IR825 nanoparticle was calculated to be 33.4%.

1.4 *In vivo* biocompatibility assessment

To systematically evaluate the *in vivo* biocompatibility of Cu-IR825 nanoparticles, hematological and histopathological analyses were performed on mice. Healthy female Balb/c mice

(16–18 g) were randomly divided into two groups, receiving either 100 μL of physiological saline (control group) or an equal volume of Cu-IR825 physiological saline dispersion (2 mg·mL^{-1}) via tail vein injection. On day 7 post-injection, mice were euthanized, blood samples were collected for biochemical analysis, and major organs were harvested for histological analysis via H&E staining.

1.5 *In vivo* photothermal imaging experiment

4T1 tumor-bearing mice were used as models. A 100 μL dispersion of Cu-IR825 nanoparticles (2 mg·mL^{-1}) was injected via tail vein. Six hours after injection, the tumor area was irradiated with an 808 nm near-infrared laser. During irradiation, infrared thermal imaging was used to monitor and record the temperature change in the tumor region over 600 seconds.

1.6 *In vivo* antitumor therapy evaluation

To systematically assess the combined therapy effect of Cu-IR825 nanoparticles *in vivo*, experiments were conducted using a 4T1 tumor-bearing mouse model. Mice were randomly divided into three groups: (1) control group (saline); (2) Cu-IR825 nanoparticle group; (3) Cu-IR825 + NIR laser group. Mice were injected with 100 μL of either physiological saline or Cu-IR825 nanoparticle dispersion (2 mg·mL^{-1}) via tail vein. Six hours after injection, tumors in group 3 were irradiated with an 808 nm near-infrared laser (1.0 W·cm^{-2}, 10 minutes). 72 hours after treatment, one mouse from each group was euthanized, and tumors were excised, fixed in 4% formaldehyde for 24 hours, embedded in paraffin, and sectioned into 4 μm thick slices. H&E staining was performed, and pathological changes in the tumor tissue were observed under an optical microscope. The remaining mice were monitored for 15 days, with body weight and tumor volume measured every 3 days. Tumor volume was calculated using the formula $V = 1/2 \times \text{length} \times \text{width}^2$ to evaluate the inhibitory effect on tumor growth by different treatments.

1.7 Biodistribution and metabolic pathway analysis

After intravenous injection of Cu-IR825 nanoparticle dispersion in mice, mice were euthanized on days 1, 5, and 15. Hearts, livers, spleens, lungs, and kidneys were harvested. Tissue samples were homogenized and digested with aqua regia for 3 days at room temperature. The samples were centrifuged, filtered through a 0.45 μm membrane, and diluted to the same volume. Copper ion content in the samples was measured using ICP-AES to analyze the distribution and temporal changes of nanoparticles in the major organs. To assess excretion pathways, mice were housed

individually in metabolic cages, and urine and feces samples were collected at different time points. After digestion with aqua regia, copper ion concentration was measured in the samples using ICP-AES to evaluate the excretion kinetics and overall clearance of the nanoparticles via urine and feces.

1.8 Statistical analysis

The data were expressed as the mean value ± standard deviation (SD), and any statistical comparison between two groups was analyzed using the Student's two-tailed test. $*p < 0.05$, $**p < 0.01$, and $***p < 0.001$.

All animal investigations conformed to the guide for the Care and Use of Laboratory Animals by the U.S. National Institutes of Health (NIH Publication no. 86-23, revised 1985) and per the protocols approved by the Animal Welfare and Research Ethics Committee of China Three Gorges University.

2. Supplementary figures

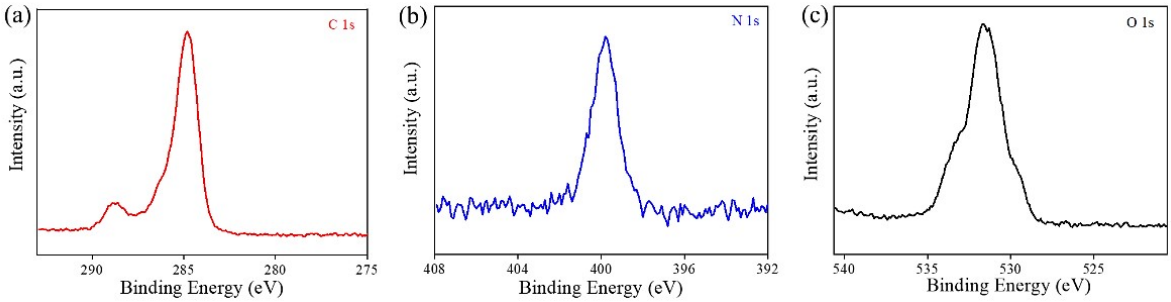

Figure S1. The C 1s, N 1s and O 1s spectra of Cu-IR825 nanoparticles.

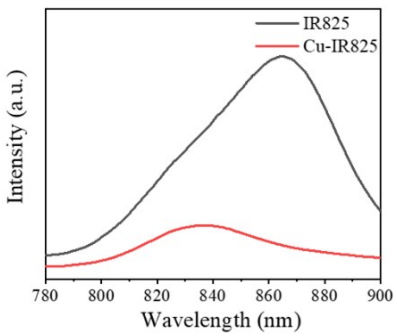

Figure S2. Fluorescence spectra of IR825 and Cu-IR825 nanoparticles.

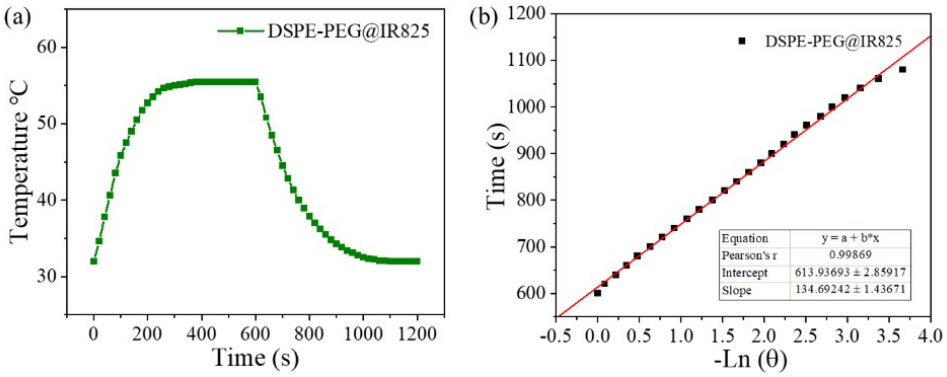

Figure S3. (a) Temperature change curves of DSPE-PEG@IR825 dispersions under laser on/off cycles. (b) Linear fitting of DSPE-PEG@IR825 data for -ln(θ) over time.

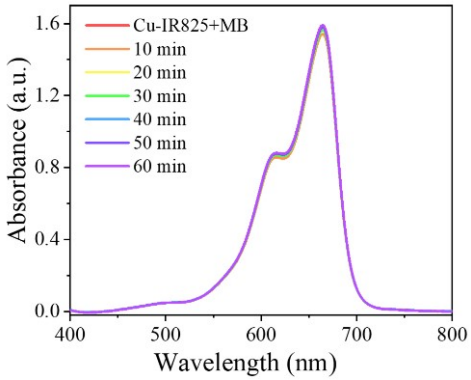

Figure S4. UV-vis-NIR absorption spectra of MB during further incubation (0–60 min) after reaching equilibrium with Cu-IR825 nanoparticles.

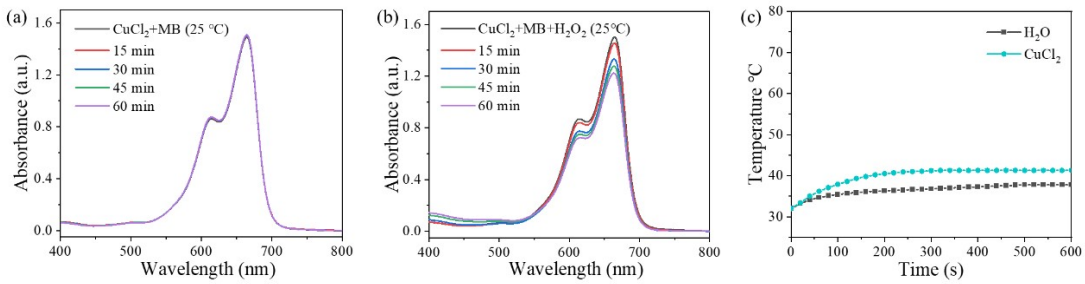

Figure S5. (a, b) Time-dependent absorption spectra of MB in $CuCl_2$ solution and/or $CuCl_2$+H_2O_2 solution at 25°C. (c) Temperature changes of $CuCl_2$ solution under 808 nm laser irradiation.

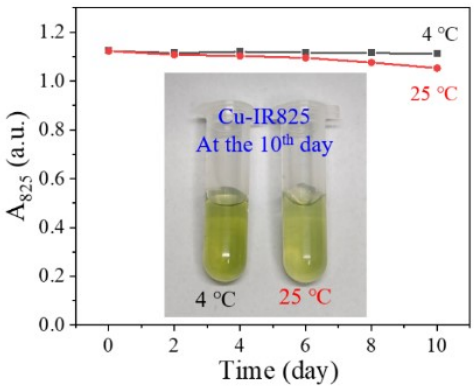

Figure S6. Time-dependent absorbance (A_{825}) of Cu-IR825 nanoparticles dispersed in PBS under different temperature conditions.

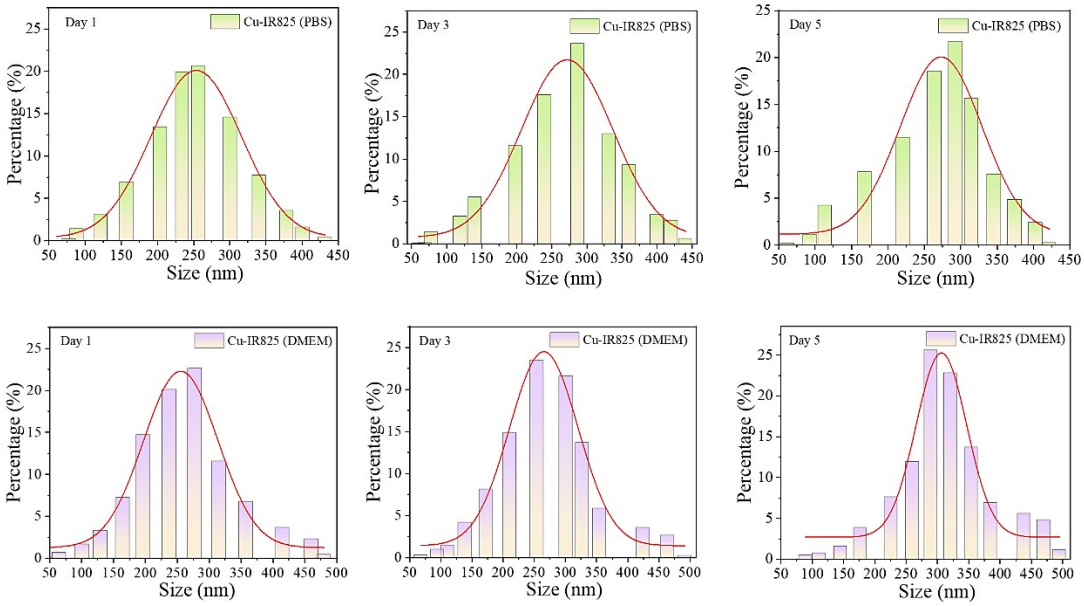

Figure S7. Time-dependent changes in the hydrodynamic diameter of Cu-IR825 nanoparticles in different biological fluids.

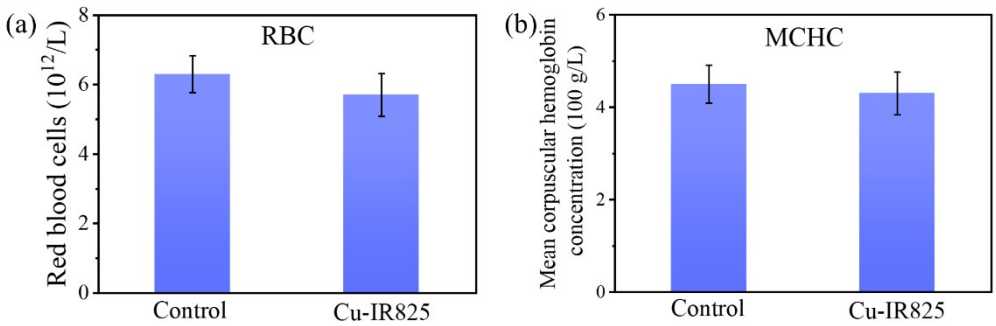

Figure S8. Blood parameters for the control and Cu-IR825 nanoparticle-treated groups on day 7.

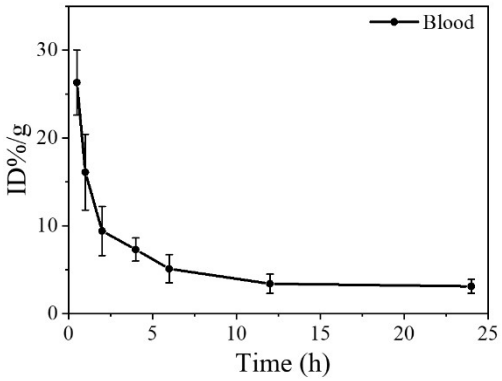

Figure S9. Pharmacokinetics of Cu-IR825 nanoparticle over a span of 24 h.

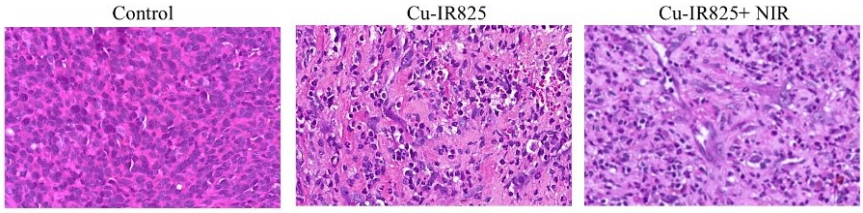

Figure S10. Images of H&E-stained tumor sections.